Fuel Processing Technology 124 (2014) 188–197

Contents lists available at ScienceDirect

Fuel Processing Technology

journal homepage: www.elsevier.com/locate/fuproc

Prediction of the combustion process in fluidized bed based on physical–chemical properties of biomass particles and their hydrodynamic behaviors

Arai A.B. Pécora [a], Ivonete Ávila [b,c], Claudio S. Lira [a], Glauber Cruz [b], Paula M. Crnkovic [b,d,*]

[a] UNICAMP — University of Campinas, School of Mechanical Engineering, 13083-860 Campinas, SP, Brazil
[b] USP — University of São Paulo, Department of Mechanical Engineering, School of Engineering of São Carlos, 13560-000 São Carlos, SP, Brazil
[c] UNESP — Univ Estadual Paulista, Department of Energy, 12516-410 Guaratinguetá, SP, Brazil
[d] UNESP — Univ Estadual Paulista, Institute of Chemistry, 14800-900 Araraquara, SP, Brazil

ARTICLE INFO

Article history:
Received 1 March 2013
Received in revised form 25 November 2013
Accepted 4 March 2014
Available online 25 March 2014

Keywords:
Biomass
Fluidized bed
Hydrodynamics
Thermal analyses

ABSTRACT

The utilization of biomass in fluidized bed reactors is due to alternatives created by the carbon credit market and to environmental concerns. This fact calls for an accurate determination of physical–chemical properties and hydrodynamic studies on biomass-inert binary mixtures. In bubbling fluidized bed combustion processes, the inert material mass is approximately 95% of the total mass of the bed material, and an effective mixture between biomass and inert particles is desired to improve the efficiency of the process. In this study, binary mixtures, composed of biomass and sand as an inert material, were used. Thermal and physical–chemical properties of five biomass samples (sugarcane bagasse, pine sawdust, coffee husk, Tucumã seed, and rice husk) were experimentally evaluated. The morphology of the samples was determined by SEM, and the thermal properties were found by thermogravimetric analysis (TG) and differential thermal analysis (DTA). The hydrodynamic study was carried out in a fluidized bed at room temperature and local atmospheric pressure, in which the minimum fluidization velocity and voidage of the biomass-inert binary mixture were evaluated. The arrangement of the physical–chemical characteristics of biomass and the hydrodynamics of the binary mixture are equally important for predictions of the biomass behavior in fluidized bed combustors.

© 2014 Elsevier B.V. All rights reserved.

1. Introduction

The increasing demand for energy has claimed for improvements in energy generation processes. The carbon credit market has created good opportunities for the use of biomass in fluidized bed reactors in industrial processes for combustion, gasification, and pyrolysis. Fluidized bed reactors are characterized by high conversion efficiencies and low emissions of atmospheric pollutants. The use of biomass in fluidized bed reactors is still restricted due to the lack of knowledge regarding biomass particle properties and their hydrodynamic behavior. Such information is important for predicting the behavior of these biomasses when they are applied to fluidized bed reactors and contributes to enhance the industrial equipment performance.

The high consumption of coal worldwide and the consequent environmental pollution problems have required the generation of a clean energy [1]. Many studies have been conducted on energy generation from biomass for environmental reasons, and fluidization is considered the most promising technology to be applied due to its good performance parameters, such as excellent fluid mixing, high heat and mass transfer rates, as well as temperature uniformity. Moreover, fluidization can operate at various regimes, depending on parameters, such as temperature, pressure, gas velocity, particle diameter, riser diameter, and gas/particles properties.

Several studies have focused on biomass particles characterization, whose knowledge is important for the improvement of the performance of such materials in thermal processes [2–7]. Within this purpose, thermal analysis techniques – thermogravimetry (TG/DTG) and differential thermal analysis (DTA) – have been used for the appraisal of the thermal behavior of the biomass providing useful information about the thermal degradation of lignocellulosic contents [8–12].

On the other hand, very few attempts have focused on the influence of physical–chemical properties of biomass materials on fluidized bed performance, probably due to the lack of sufficient data on those properties. Regarding binary mixtures involving biomass and sand particles, an effective mixture inside the bed must be achieved for a better

---

[*] Corresponding author at: Department of Mechanical Engineering, USP, University of São Paulo, Av. Trabalhador São Carlense, 400, CEP 13566-590 São Carlos, SP, Brazil. Tel.: +55 16 31161665.

E-mail addresses: paulam@sc.usp.br, paulamcrn@gmail.com (P.M. Crnkovic).

http://dx.doi.org/10.1016/j.fuproc.2014.03.003
0378-3820/© 2014 Elsevier B.V. All rights reserved.

performance of the reactor [13]. However, more experimental studies on the hydrodynamic behavior of fluidized beds containing binary mixtures of biomass and sand particles are still required, although plenty of research has been carried out over the past four decades [14–17].

These studies have shown that the values provided by equations of the minimum fluidizing velocity (U_{mf}) for binary mixtures with biomass particles are far from the experimental ones due to the segregation phenomena, irregular shapes of biomass and the formation of preferential channels inside the bed. Despite all efforts devoted, the combination between hydrodynamic studies of biomass-sand mixtures in fluidized beds and studies on physical–chemical properties of biomass still have not been analyzed.

In this context this paper investigates five biomass samples (sugar cane bagasse, pine sawdust, coffee husk, Tucumã seed and rice husk) based on the thermal and physical–chemical properties and hydrodynamic behavior of biomass–sand binary mixtures. The fluidization process of the binary mixture in the fluidized bed is conducted by using air at room temperature and local atmospheric pressure. The arrangement of the physical–chemical properties of biomass and hydrodynamic behavior enables the prediction of the fluidized bed combustors when the biomass is used. Such attempts are expected to lead to a better utilization of the biomass samples in thermal processes.

2. Materials and methods

2.1. Solid particles

The five biomass samples studied were collected from different regions in Brazil: sugarcane bagasse, pine sawdust, and coffee husk from São Paulo State, Tucumã seed from Amazonas State and rice husk from Maranhão State. All biomass particles were ground by either a hammer mill or a slicer to obtain particle sizes smaller than 2800 μm, except for rice husk. This preparation followed the ASTM Standards (E1757-01).

Sand particles whose size ranged between 150 μm and 1000 μm were selected for hydrodynamic experiments and subjected to both particle and bulk density experimental analyses. However, smaller particles were required for porosimetry and thermal analyses. In those cases, particles of 460 μm were used, but previously washed, dried at 80 °C for 18 h, grounded, and then sieved. The average size of 460 μm was obtained by the arithmetic mean of two consecutive ASTM laboratory sieves whose mesh apertures ranged between 420 and 500 μm. Pictures of the biomass samples after the preparation are shown in Fig. 1.

2.2. Physical–chemical analyses

Ultimate analysis, higher heating value (HHV) and porosity tests were carried out to characterize the biomass samples. The ultimate analysis of the samples was conducted with a CE Instruments analyzer — model EA1110-CHNS-O. HHV was determined on a bomb calorimeter (IKA C200) according to the ASTM D-2015 standard test method and using samples weighing (1.0 ± 0.1)g in three replicate experiments.

The samples were dried in an oven for approximately 24–120 h under a temperature of 110 °C prior to the porosimetry tests conducted in a Micromeritics porosimeter (ASAP-2020). Samples of (1.0 ± 0.3)g were used in all experiments. Under the Degas conditions, the samples were heated at a 10 $°C\,min^{-1}$ up to 70 °C rate and subjected to an evacuation rate of 10 $mmHgs^{-1}$ to 10 μmHg, remaining under these conditions for 240 min. Under the analysis conditions, the samples were immersed in liquid nitrogen and maintained in isothermal conditions at −196 °C during all experiments. The porosimetry analysis was performed under vacuum at an evacuation rate of 5 $mmHgs^{-1}$ to 10 μmHg, remaining under these conditions for 6 min. Then, a P/P_0 programming for 42 points was applied (27 points for adsorption and 15 points for desorption). P/P_0 is the ratio between the applied pressure (P) and the saturation vapor pressure of the adsorbed gas (P_0), i.e., nitrogen.

The morphological structures of the biomass samples were analyzed by Scanning Electron Microscope (SEM) in a LEO Electron Microscopy 440 (ZEIZ/LAIKA).

2.3. Thermal analyses

The thermal properties of the samples were determined by both thermogravimetric analysis (TGA) and differential thermal analysis (DTA). The TG technique determines the changes in the sample mass as the temperature increases and DTA determines the enthalpic transitions by means of endothermic and exothermic peaks [18]. The experiments were performed in a thermogravimetric balance and in a

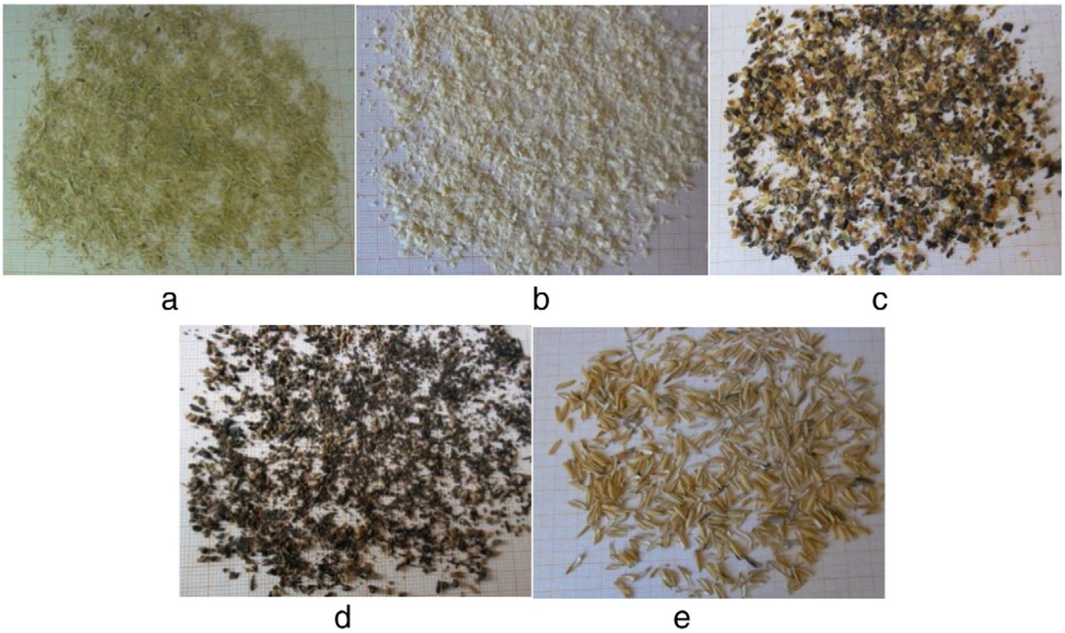

Fig. 1. Samples of the five biomasses studied: (a) sugarcane bagasse; (b) pine sawdust; (c) coffee husk; (d) Tucumã seed and (e) rice husk.

differential thermal analyzer under the following conditions: sample mass of (10 ± 0.3)mg placed inside an alumina crucible and heating rate of 10 °C min^{-1} (from room temperature up to 700 °C) under synthetic air atmosphere at flow rate of 100 mL min^{-1}. The thermogravimetric equipment was calibrated previously and experiments were run twice to verify repeatability. Average particle sizes of 545 μm were used for the TG and DTA analyses.

2.4. Physical properties

The volume-surface average particle diameter, or Sauter mean diameter ($\overline{d}_p$), for the inert material (sand) and for each biomass was determined by sieving analysis using standard mesh sizes according to the American Society of Testing Materials (ASTM).

The mean volume-surface particle diameter, calculated by Eq. (1), was used as it is based on the specific surface area per unit volume of the particles, which is more recommended to fluidized bed systems,

$$\overline{d}_p = \frac{1}{\sum_i x_i d_{pi}}. \tag{1}$$

The particle densities (ρ_p) were measured by liquid picnometry using n-heptane as displacement fluid and the bulk density for each material (ρ_{bulk}) was obtained from mass and volume measurements of the loosely packed bed contained in a vessel of 0.2 m diameter and 0.2 m height in order to reduce wall effects. The bulk voidage under the minimum fluidization condition (ε_{mf}) was estimated from Eq. (2), assuming that ε_{mf} is very close to the voidage of the loosely packed bed for group B particles according to Geldart classification [19],

$$\varepsilon_{mf} = 1 - \frac{\rho_{bulk}}{\rho_p}. \tag{2}$$

The particle diameter and the solid density of the binary mixture were obtained by Eqs. (3) [14] and (4) [5].

$$\frac{1}{d_{p,mix}} = \frac{x_B}{d_{p,B}} + \frac{(1-x_B)}{d_{p,S}} \tag{3}$$

$$\rho_{p,mix} = x_B \rho_{p,B} + (1-x_B)\rho_{p,S} \tag{4}$$

where subscripts mix, B and S refer to binary mixture, biomass and sand particles, respectively.

The biomass mass fraction (x_B) was defined by Eq. (5), from biomass and sand weights inside the bed (M_B and M_S).

$$x_B = \frac{M_B}{M_B + M_S}. \tag{5}$$

2.5. Hydrodynamic study of biomass–sand binary mixtures

This study involves the determination of a minimum fluidization velocity of the biomass–sand binary mixtures composed of 95% of sand (weight fraction) and 5% of biomass. The experiment was also conducted using only sand particles as the bed material in order to obtain the minimum fluidization velocity of the inert material.

The tests were carried out in a laboratory scale fluidized bed system schematically shown in Fig. 2. The riser (0.1 m internal diameter, 2.5 m height) was built by sections of glass (borosilicate), acrylic and steel, enabling the visualization of the operational regime. A perforated plate (0.001 m orifice diameter, 0.008 m pitch, 1.3% open area) was used as a gas distributor and the height of the loosely packed bed was fixed at 0.10 m. The air flow at room temperature was provided by a blower (36 kPa maximum pressure and 0.1 $m^3 s^{-1}$ maximum air flow). An orifice plate, built under the specifications of ASME MFC-14M-2003, and a

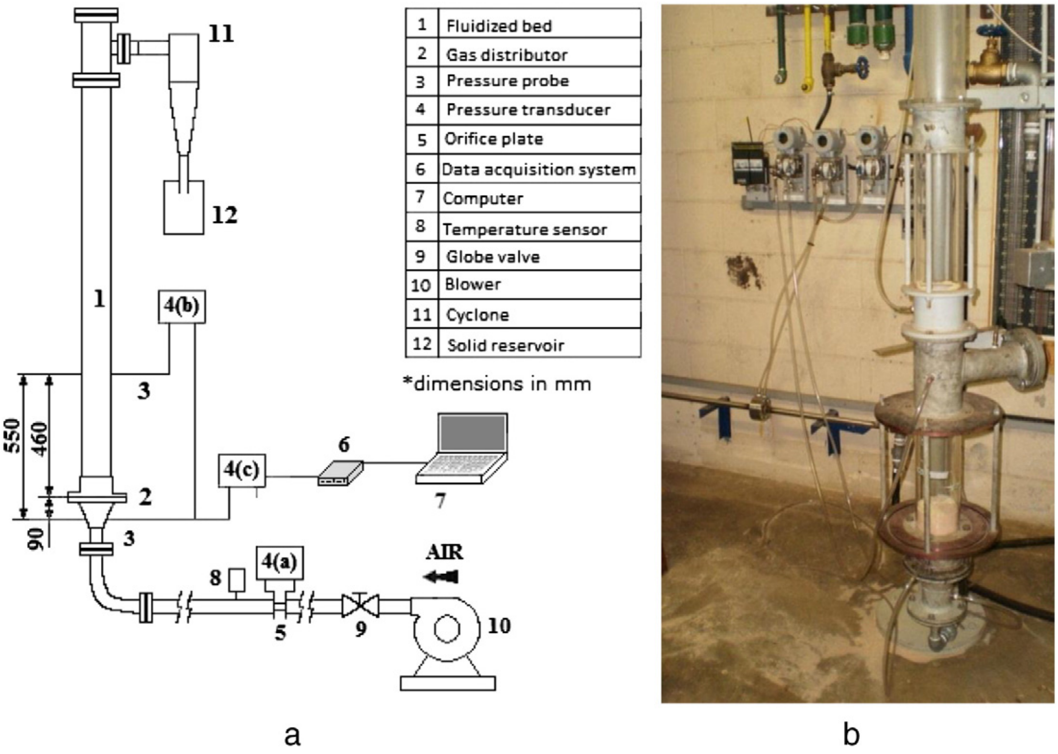

Fig. 2. Experimental system: (a) schematic and (b) image of the laboratory-scale fluidized bed system.

differential pressure transducer enabled the determination of the air flow rate. A Lapple cyclone collected the entrained particles in the solids reservoir.

The bed pressure drop was measured in the plenum by a differential capacitive pressure sensor (SMAR model LD301, ranging from 0 to 50 kPa, with 4-to-20 mA DC loop current). The uncertainty of the pressure measurements of approximately 1 Pa was obtained by calibration using a U-type manometer and a multimeter, both previously calibrated and certified. Additionally, a slender material filter was used to avoid the pressure probe obstruction.

The minimum fluidization velocity was experimentally obtained by pressure drop measurements through the bed (ΔP_{bed}) as a function of superficial gas velocity (U).

At the beginning of each test, the bed was filled with the previously mixed binary mixture and the air flow rate was increased from zero up to the bubbling fluidized bed regime. The air flow rate was then reduced to zero. The bed pressure drop (ΔP_{bed}) was measured at each successive flow rate reduction.

For each biomass–sand mixture, five experiments were conducted to obtain the hydrodynamic curve and then the $\mathrm{U_{mf}}$ of the binary mixture.

Due to the onset of preferential channels, or plug flow behavior, hydrodynamic tests using only biomass particles as the bed material could not be conducted. The theoretical prediction of the biomass minimum fluidized velocity ($\mathrm{U_{mf}}$) was based on Ergun's equation, as recommended by Rowe [20] for pressures up to 100 bar. Eq. (6) shows this expression in terms of operating variables.

$$\mathrm{U_{mf}} = \frac{\mu}{\rho d_p} 42.9\left(1-\varepsilon_{mf}\right)\left\{\left[1+3*10^{-4}\frac{\varepsilon_{mf}^3}{\left(1-\varepsilon_{mf}\right)^2}Ar\right]^{1/2}-1\right\}. \tag{6}$$

The Archimedes number (Ar) is given by Eq. (7),

$$Ar = \frac{d_p^3\rho\left(\rho_p-\rho\right)g}{\mu^2} \tag{7}$$

where μ and ρ are the dynamic viscosity and density of the air, respectively, and g is the gravitational acceleration.

Regarding the biomass binary mixture (B) and sand (S), Eq. (8) [16] can be used to estimate the minimum fluidized velocity of the mixture ($\mathrm{U_{mf,mix}}$) based on the mass fraction of the biomass in the bed.

$$\mathrm{U_{mf,mix}} = x_\mathrm{B}U_{mf,\mathrm{B}} + (1-x_\mathrm{B})\cdot U_{mf,\mathrm{S}}. \tag{8}$$

3. Results and discussion

This section describes the results of two strands. The first is related to the physical–chemical and thermal evaluations of the biomass, while the second refers to the hydrodynamic studies performed in a fluidized bed under room temperature and local atmospheric pressure.

Table 1
Ultimate analyses and higher heating values (HHV).

Biomass	Ultimate Analysis (wt.% on a dry, ash-free basis)					HHV (dry basis) (MJ/kg)
	C	H	N	S	O	
Sugarcane bagasse	45.05	4.86	0.25	nd	38.54	17.47 ± 0.10
Pine sawdust	46.60	5.37	0.40	nd	39.23	18.32 ± 0.18
Coffee husk	43.13	5.02	1.55	0.67	33.13	16.79 ± 0.07
Tucumã seed	48.83	6.12	0.88	nd	33.57	20.78 ± 0.07
Rice husk	39.11	4.12	0.31	0.59	37.57	15.39 ± 0.11

3.1. Physical–chemical and thermal analyses

The results of the ultimate analyses and the high heating value (HHV) are provided in Table 1.

The Tucumã seed exhibited the highest C and H content, hence the highest HHV. Rice husk exhibited the lowest HHV followed by coffee husk. Comparing the results in Table 1, the HHV values are directly proportional to the C and H content of the biomass.

Table 1 also shows that coffee and rice husks have 0.67% and 0.59% sulfur content, respectively. As expected, the sulfur content in the biomass is lower than 0.2% [20], which indicates these materials should be treated with great caution, due to the emission of pollutant gas ($\mathrm{SO_x}$) and corrosion problems of the equipment.

Among the biomass samples in this study, only the N content of coffee husk is higher than 1%, therefore its contribution to $\mathrm{NO_x}$ emission from combustion processes will be higher than the contribution of the others. This is an important issue to be considered because the $\mathrm{NO_x}$ formation depends on both fuel and thermal conditions. Thermal $\mathrm{NO_x}$ has a significance at temperatures above 1540 °C [21–23]. In fluidized beds, the combustion occurs at temperatures between 850 °C and 950 °C and, consequently, the thermal $\mathrm{NO_x}$ production is not significant in these combustion processes. However, Qian et al. [24] reported results of high nitrogen content biomass emissions in a pilot-scale vortexing fluidized bed combustor and concluded that there is no obvious relation between NO emission and fuel-N content. They speculated that the chemical structure of the fuel may be an important factor that should also be evaluated.

The porosity effect was described as an important parameter that affects the conversion progress of the particle [25]. The surface area was obtained from the polynomial form of BET equation (Brunauer, Emmett and Teller). The BJH method (Barrett, Joyner and Halenda) was applied to determine the average pore diameter and the cumulative volume of pores.

Fig. 3 shows the nitrogen adsorption/desorption isotherms for the five biomass samples and Table 2 provides the average values of BET surface area ($\mathrm{S_{BET}}$), BJH desorption average pore diameter ($\mathrm{D_{BJH\,\cdot\,Des}}$), BJH desorption cumulative volume of pores ($\mathrm{V_{BJH\,\cdot\,Des}}$), and values of the maximum quantity of adsorbed gas ($\mathrm{Q_A}$). As the standard deviations provide low values, porosimetry experiments are supposed to have good reproducibility.

Type IV shape of the isotherm for rice husk and Tucumã seed indicates that these materials are mesoporous solids [26], and the presence of hysteresis confirms the difference in the absorption and desorption mechanisms of nitrogen for all samples. For the coffee husk, Pinus sawdust and sugar cane bagasse, there is no hysteresis, which indicates they are very low porous materials. As shown in Fig. 3 and Table 2 rice husk adsorbed the highest amount of nitrogen ($\mathrm{Q_A}$) representing a total volume of $(3.99 \pm 0.36)\mathrm{cm^3\,g^{-1}}$. On the other hand, coffee husk adsorbed the lowest volume of nitrogen $(0.93 \pm 0.03)\ \mathrm{cm^3\,g^{-1}}$. All such values are very low and characterize low-porosity materials.

The surface area of the biomass samples ranges between 0.26 and 0.69 $\mathrm{m^2\,g^{-1}}$ and the average pore diameter between $(87.6 \pm 20.6)\mu\mathrm{m}$ and $(228.9 \pm 3.4)\mu\mathrm{m}$. These results show the very low porous structure of the biomass particles. Among the biomass samples studied, rice husk has shown the highest $\mathrm{S_{BET}}$ value and also the highest porosity level, as evidenced by the $\mathrm{D_{BJH\,\cdot\,Des}}$ and $\mathrm{V_{BJH\,\cdot\,Des}}$ values. However, coffee husk has shown the lowest $\mathrm{S_{BET}}$ value, but a high pore diameter ($\mathrm{D_{BJH}}$). The results have confirmed the non-microporous nature of the biomass samples, whose surface area and pore volumes may be attributed to mesopores and macropores. Fig. 4 shows the distribution of pore sizes for all biomass samples. Except for rice husk, which has macropores (pores or slits of diameters larger than 500 Å), the other biomasses have only mesopores (between 2 Å and 500 Å) [27].

The literature still lacks results which shows the pore size characteristics and the behavior of isotherms adsorption/desorption for different biomasses. These materials have different characteristics, therefore a

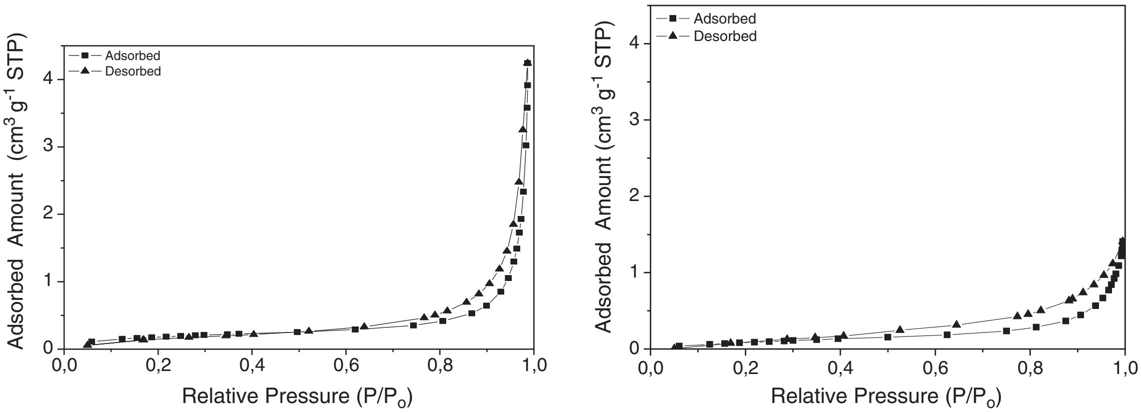

Rice husk

tucumã seed

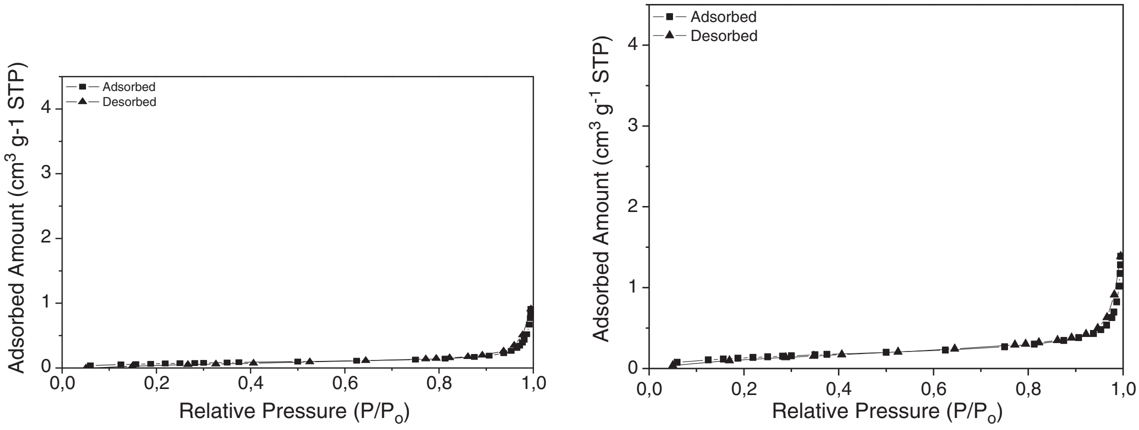

Coffee husk

Pinus sawdust

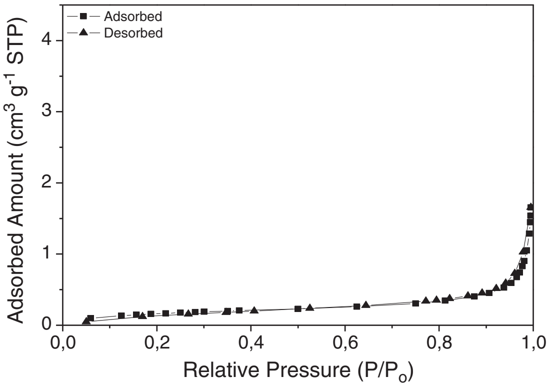

sugar cane bagass

Fig. 3. Nitrogen adsorption and desorption isotherms of biomass materials.

Table 2
Porosity characteristic of the biomass samples determined by nitrogen gas adsorption.

Biomass	Drying time (h)	Sample mass (mg)	S_{BET} ($m^2\ g^{-1}$)	$D_{BJH\ \cdot\ Ds}$ (4 V/A) (μm)	$V_{BJH\ \cdot\ Ds}$ $\times 10^3$ (μm)	Q_A ($cm^3\ g^{-1}$ SPT)
Sugarcane bagasse	24	1.47 ± 0.04	0.63 ± 0.01	146.4 ± 27.1	2.10 ± 0.48	1.43 ± 0.32
Pine sawdust	24	1.94 ± 0.01	0.47 ± 0.08	164.4 ± 2.1	1.69 ± 0.48	1.16 ± 0.32
Coffee husk	48	2.01 ± 0.01	0.26 ± 0.02	201.0 ± 12.6	1.40 ± 0.03	0.93 ± 0.03
Tucumã seed	120	1.46 ± 0.01	0.41 ± 0.03	87.6 ± 20.6	1.94 ± 0.24	1.60 ± 0.28
Rice husk	24	1.25 ± 0.29	0.69 ± 0.00	228.9 ± 3.4	6.10 ± 0.58	3.99 ± 0.36

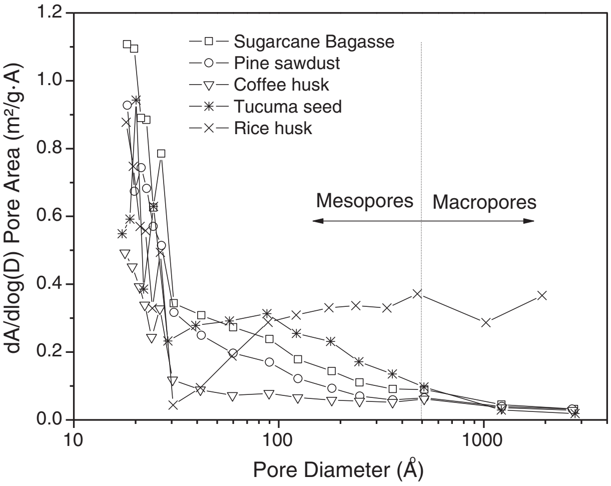

Fig. 4. Pore size distributions obtained by nitrogen adsorption of biomass materials.

specific methodology must be developed for each biomass involving sample mass and the drying time required. As shown in Table 2, the mass ranged from 1.25 to 2.01 mg and the drying time from 24 to 120 h, depending on the biomass, i.e., for each biomass there is a specific condition, which provides a more reliable result.

Distinguishable morphological structures can be evidenced from the SEM images shown in Fig. 5 obtained for the five biomass particles studied. Those images have revealed the essentially non-porous structure of the biomass.

The SEM image for the sugarcane bagasse, Fig. 5(a), shows elongated cylindrical fiber shapes. This characteristic was previously observed for the fibrous fraction of sugarcane of size particles of 1.00 mm that was milled in a cutting mill [28]. The SEM images obtained from pine sawdust, Fig. 5(b), and coffee husk, Fig. 5(c), show similar characteristics in their morphological surface structure and a structure with high surface disorder and also flat shaped elements. However, coffee husk has a more compacted and heterogeneous surface than pine sawdust. For Tucumã seed, Fig. 5(d), a variety of cavities in a longitudinal and a well-organized porous structure can be observed. Fig. 5(e) shows the morphological surface of rice husk, in which highly ordered fibrils can be observed [29,30]. The SEM images have confirmed the very low porous nature and the different morphologies of those materials. Such information provides subsidies to understand biomasses exhibiting different morphologies.

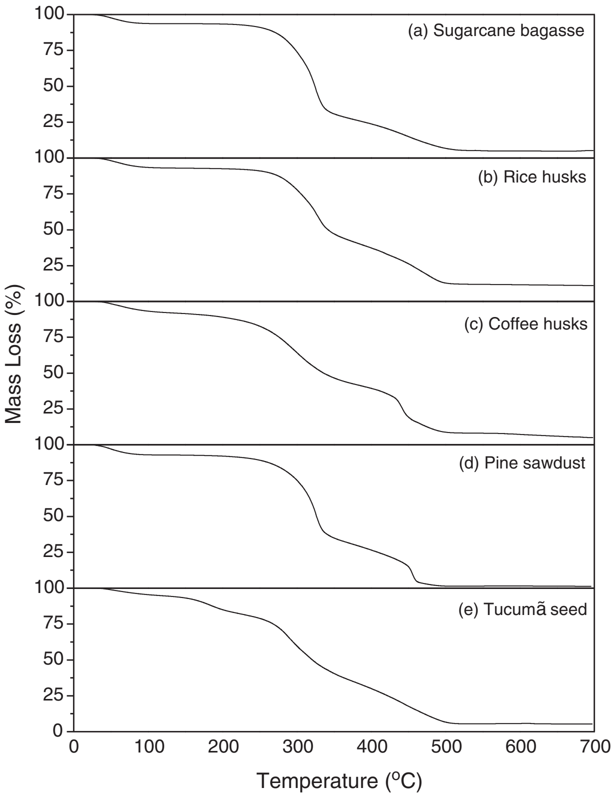

Fig. 6. TG curves versus temperature (synthetic air atmosphere, heating rate of 10 °C min^{-1}, flow rate of 100 mL min^{-1}). Mass loss for all curves ranged from 0 to 100%.

Figs. 6 to 8 show thermogravimetric, derivative thermogravimetric and differential temperature curves, respectively, for all samples.

For each sample, the thermal decomposition proceeded within three regions, which correspond to the main components of the biomass.

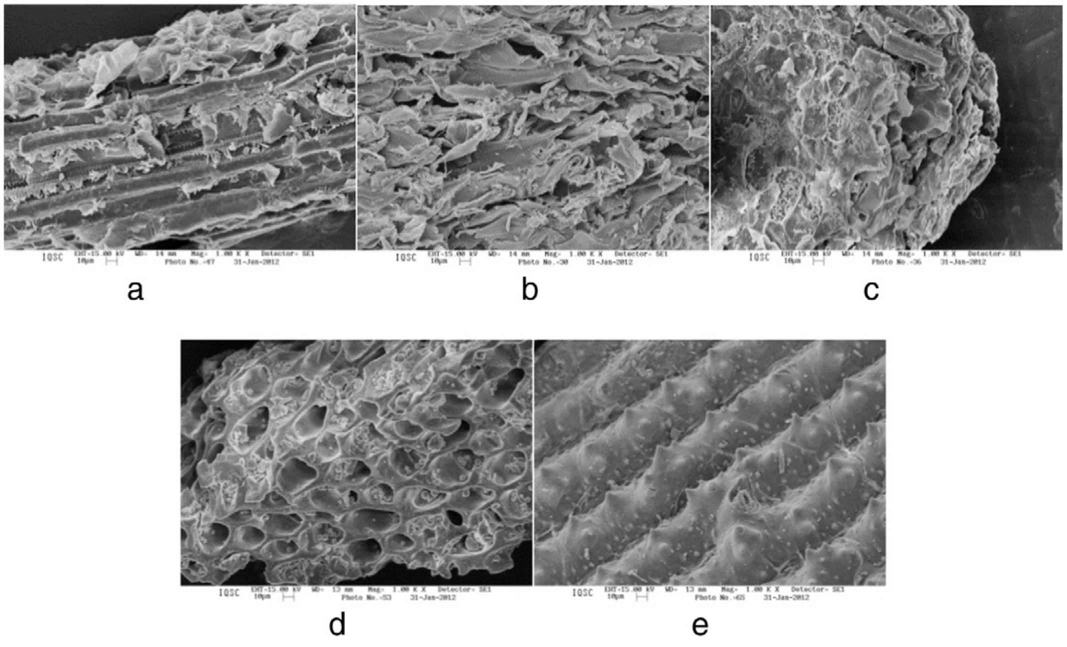

Fig. 5. SEM micrograph of the five biomass samples (amplitude of 1000×): (a) sugarcane bagasse (b) pine sawdust, (c) coffee husk, (d) Tucumã seed and (e) rice husk.

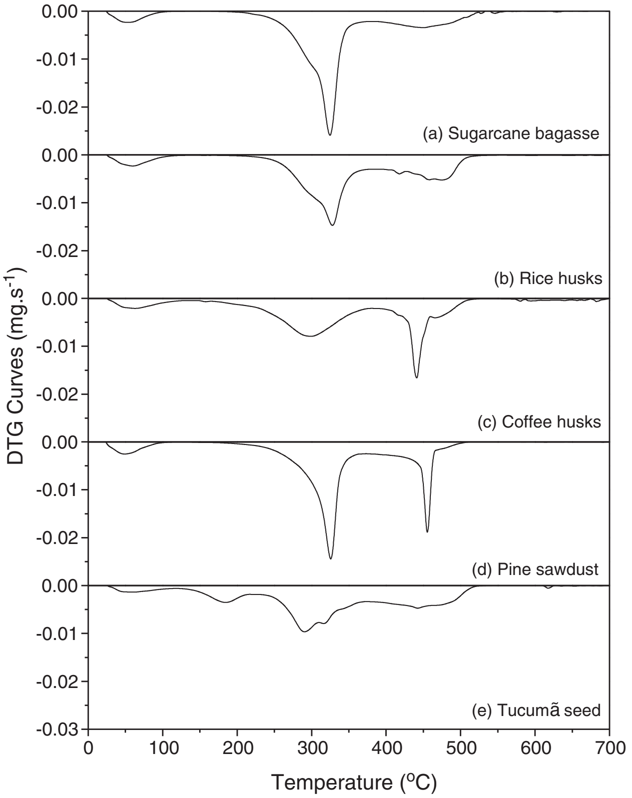

Fig. 7. DTG curves versus temperature (synthetic air atmosphere, heating rate of 10 °C min^{-1}, flow rate of 100 mL min^{-1}). All DTG curves ranged from −0.03 to 0.00 mg s^{-1}.

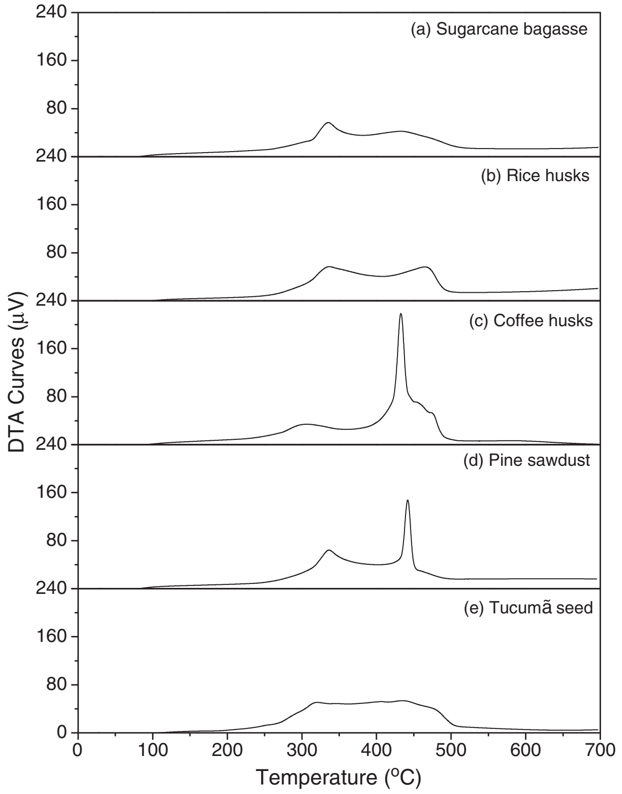

Fig. 8. DTA curves versus time (synthetic air atmosphere, heating rate of 10 °C min^{-1}, flow rate of 100 mL min^{-1}). All DTA curves ranged from 0 to 240 µV.

Step 1 is related to moisture content. Although all samples were dried prior to analyses, moisture is still present due to the hydrophilic nature of the biomass particles. The second step (from 120 °C up to 445 °C, depending on the biomass) is related to cellulose and hemicellulose contents. The third step of degradation is the result of the lignin present in the biomass particles. Lignin decomposes at a longer time since it is resistant until 514 °C–550 °C, depending on the biomass type. Although the temperature decomposition slightly depends on the heating rate used, when temperatures higher than 550 °C are applied, the total biomass decomposition is ensured, even in reactors.

The temperature ranges for each degradation step are provided in Table 3 for all samples, and the results are consistent with those found in the literature related to the assessment of combustion [12] and pyrolysis [31] processes.

Table 3 also includes the mass loss for each step and ash content obtained at the end of the TG experiment. It is noteworthy that the burnout temperature corresponds to the final temperature of the third event. The TG results showed good reproducibility due to the low standard deviation values obtained from the mass loss results.

DTA curves show the enthalpic events for each step. For all samples, there is one endothermic peak associated with the moisture content and two exothermic peaks (the first is higher than the second for sugarcane bagasse, Tucumã seed and rice husk). For pine sawdust and coffee husk, a different behavior is observed, i.e., the second exothermic peak is higher than the first, therefore, a correlation with DTG curves for these steps can be established. The two exothermic events correspond to the DTG peaks; as for sawdust and coffee husk samples, the intensity of the second peak is higher than the intensity of the first.

From DTA curves, the peak at around 300 °C can be related to the decomposition of cellulose and hemicellulose content in all samples. This step corresponds to an exothermic event and, according to Shen et al. [32] the second step (hemicellulose and cellulose decomposition) is related to devolatilization, which enables the release of volatiles and char formation. Subsequently, char reacts with oxygen resulting in the combustion process. Although the formation of volatiles is an endothermic event, exothermicity predominates as a result of devolatilization and combustion.

3.2. Hydrodynamic study

Table 4 shows the properties of the biomass and sand particles used in the hydrodynamic experiments. The physical properties of the solid particles are mean Sauter diameter ($\bar{d}_p$), particle density (ρ_p), bulk density (ρ_{bulk}) of the loosely packed bed, and bulk voidage under minimum fluidization condition (ε_{mf}). These values represent the average of at least three replicates. The value of superficial gas velocity estimated under the minimum fluidization condition (U_{mf}) for each material using Eq. (6) is also shown in Table 4.

The rice husk particles showed the highest average diameter, which explains the high U_{mf} value for this biomass (Table 4). Comparing the pair of samples sugarcane bagasse/Tucumã seed and pine sawdust/coffee husk, as each pair has an equivalent average diameter, the influence of the bulk voidage on the minimum fluidization velocity can be noticed. Results show that a higher value of ε_{mf} results in a higher U_{mf} value, predicted from Eq. (6). This fact can be explained by the higher interstitial volume among particles in a bed of higher bulk voidage, which enables the gas to flow through the bed easily. Therefore, the particles are suspended by the gas only at higher velocities.

The hydrodynamic curves (ΔP_{bed} versus U) of typical tests involving a bed composed of 5% of biomass (weight fraction) and sand are shown in Fig. 9 for each binary mixture studied. The lowest bulk density of the rice husk–sand mixture resulted in a small quantity of material in the bed, whose height was fixed at 0.10 m. This fact explains the low value of bed pressure drop when this biomass is present.

Higher hysteresis, characterized by the difference between the up flow and the down flow results (indicated by arrows in Fig. 9) was

Table 3
Temperature range and percent mass loss observed at each step of thermal degradation for all biomasses.

Biomasses	Degradation steps	Temperature (°C)	Peak temperature (°C)	Mass loss (%)
Sugarcane bagasse	1	25–105	–	6.4 ± 0.2
	2	200–375	326	67.7 ± 1.4
	3	375–550	442	20.9 ± 0.7
	Ash	>550	–	4.8 ± 1.9
Pine sawdust	1	25–105	–	7.2 ± 0.1
	2	170–380	331	61.8 ± 0.2
	3	380–520	456	29.6 ± 0.0
	Ash	>520	–	1.2 ± 0.0
Coffee husk	1	25–105	–	8.2 ± 0.3
	2	150–445	302	73.7 ± 3.6
	3	445–520	439	10.0 ± 1.1
	Ash	>520	–	8.3 ± 2.8
Tucumã seed	1	25–105	–	5.3 ± 0.3
	2	120–380	297	60.7 ± 0.7
	3	380–530	456	28.9 ± 0.6
	Ash	>530	–	5.3 ± 0.4
Rice husk	1	25–105	–	7.1 ± 0.4
	2	200–337	329	53.3 ± 1.3
	3	375–514	472	27.6 ± 0.3
	Ash	>514	–	11.2 ± 2.4

Table 4
Properties of the solid particles: biomass and sand particles.

Solid particles	$\bar{d}_p \times 10^6$ (m)	ρ_p (kg m^{-3})	ρ_{bulk} (kg m^{-3})	ε_{mf} (−)	U_{mf} [Eq. (6)] (m s^{-1})
Sugarcane bagasse	242 ± 5	953 ± 97	114 ± 2	0.88 ± 0.01	0.582 ± 0.055
Pine sawdust	529 ± 21	1366 ± 142	137 ± 2	0.90 ± 0.01	1.423 ± 0.100
Coffee husk	570 ± 10	1361 ± 55	470 ± 7	0.66 ± 0.01	0.675 ± 0.038
Tucumã seed	256 ± 8	1195 ± 155	516 ± 4	0.57 ± 0.06	0.111 ± 0.050
Rice husk	1590 ± 50	1089 ± 90	114 ± 3	0.90 ± 0.01	2.325 ± 0.122
Sand	293 ± 7	2622 ± 16	1517 ± 25	0.42 ± 0.01	0.098 ± 0.009

verified for sugarcane particles. This behavior could be attributed to the high concentration of fine particles and non-uniformity shape of this biomass sample, which indicates that the particles are reorganized in the fluidization process. Due to these characteristics of the bagasse, more control on the fluidization process is required in relation to other biomass materials studied. Bagasse exhibited a higher tendency of segregation, i.e., there was more accumulation of biomass at the upper region of the bed while the sand was deposited at the bottom of the column.

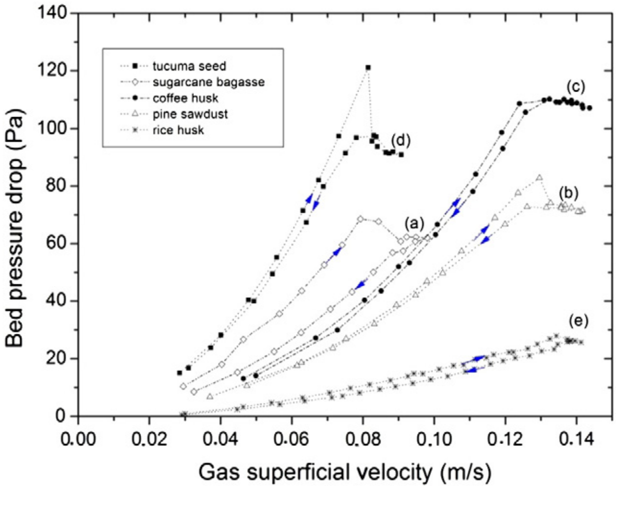

Fig. 9. Hydrodynamic curves for the five binary mixtures (5% weight fraction of biomass in the bed): (a) sugarcane bagasse; (b) pine sawdust; (c) coffee husk; (d) Tucumã seed and (e) rice husk.

The properties of the binary mixtures studied and the experimental minimum fluidization velocity ($U_{mf,mix}$) are shown in Table 5. The minimum fluidization velocities were obtained from the intersection of the pressure drop line of the fixed bed with that of the initial fluidization state. The $U_{mf,mix}$ predicted values from Eq. (8) are also provided in Table 5.

Small differences were observed among the binary mixtures studied regarding average particle size and density of the bed containing 5% of biomass (weight fraction), as the sand material is the main component inside the bed. However, U_{mf} experimental values (Table 5) varied from 0.076 m s^{-1} (tucumã seed–sand mixture) to 0.129 (rice husk–sand mixture), showing that the minimum fluidization velocity of the binary mixture depends on the biomass properties. These results show that even a small quantity of biomass leads to a strong influence on the bed hydrodynamics. The U_{mf} experimental results for pine sawdust–sand, coffee husk–sand and rice husk–sand mixtures were similar (0.126 to 0.129 m s^{-1}), which suggests that there is a compensation of particle diameter, density and voidage influences on particle–particle and particle–gas interactions.

The bulk density of the binary mixture, shown in Table 5, explains the different weights of the bed materials inside the system depending on the biomass type, as the bed height was fixed at 0.10 m. A higher bulk density implies a heavier bed, hence a weight and a higher pressure drop at a fluidized bed regime (Fig. 9).

Theoretical values of minimum fluidization velocity ($U_{mf,mix}$) obtained through Eq. (8) revealed deviations from 1 to 63% related to experimental values, showing that this equation must be cautiously used to predict U_{mf} values for biomass–sand mixtures. The highest deviation

Table 5
Properties of the biomass–sand mixture (5% weight fraction of biomass).

Biomass in the binary mixture	$d_{p,mix} \times 10^6$ (m) [Eq. (3)]	$\rho_{p,mix}$ (kg m^{-3}) [Eq. (4)]	$\rho_{bulk,mix}$ (kg m^{-3})	Experimental $U_{mf,mix}$ (m s^{-1})	$U_{mf,mix}$ (m s^{-1}) [Eq.(8)]
Sugarcane bagasse	290 ± 7	2539 ± 23	1165 ± 20	0.085 ± 0.006	0.122 ± 0.010
Pine sawdust	300 ± 7	2559 ± 21	1175 ± 18	0.128 ± 0.007	0.165 ± 0.017
Coffee husk	300 ± 7	2559 ± 20	1445 ± 15	0.126 ± 0.010	0.127 ± 0.010
Tucumã seed	291 ± 7	2551 ± 22	1586 ± 15	0.076 ± 0.001	0.099 ± 0.009
Rice husk	305 ± 8	2545 ± 22	992 ± 22	0.129 ± 0.009	0.210 ± 0.026

between experimental and predicted U_{mf} values was obtained for rice husk and the lowest for Tucumã seed, which suggests that small deviations occur when the biomass and the inert material show similar U_{mf}.

3.3. Effect of the physical properties of the biomass particles on their hydrodynamic behavior

Experimental results, shown in Fig. 9, indicate that the binary mixture with Tucumã seed and sugarcane bagasse reached the regime of bubbling fluidized bed at a lower gas velocity than the regimes obtained for the mixtures with other biomass samples.

A lower minimum fluidization velocity represents an advantage regarding energy consumption by blowers or compressors used in fluidized beds. The particle size influenced this result, as Tucumã seed and sugarcane bagasse showed a lower Sauter diameter mean value than the other biomass particles.

The bed pressure drop is an important prediction in the design of fluidized bed systems, as it is related to the energy required by the air injection equipment. For a fixed bed height, a binary mixture with a lower bulk density supports a lower bed weight, as showed by the rice husk–sand mixture. Therefore, both individual biomass particle and binary mixture properties must be observed for a good fluidized bed reactor design.

3.4. Assessment of the morphological and thermal characteristics of the biomass samples

No obvious correlation between the thermal behavior of the samples and their physical structure (S_{BET}, $D_{BJH\ \cdot\ Ds}$, $V_{BJH\ \cdot\ Ds}$ and Q_A) has been observed, but a trend could be established with their morphological structure. SEM images of coffee husk and pine sawdust exhibited a more disordered structure than the other samples, as previously described. For these samples, in both DTA and DTG curves, the second peak is higher than the first (Figs. 7 and 8). As aforementioned, the first peak, in both DTA and DTG curves, is related to the hemicellulose and cellulose decomposition, and the second to lignin. In samples in which the second peak is more intense than the first, this may be a consequence of the lignin more loosely attached in the lignocellulosic structure. Possibly, the disorder observed in the coffee husk and pine sawdust makes their structures more fragile, causing more accessibility of the oxygen into the internal sites and resulting in a very good combustion reaction.

Due to the lignocellulosic nature of the biomass, it is possible to predict that inside a fluidized bed combustion chamber, besides hydrodynamic behavior, the thermal properties strongly affect the system regarding combustion kinetics, emissions, entrainment, and particles agglomeration.

4. Conclusions

The evaluation of the thermal properties of the biomass samples by TG/DTG and DTA complemented by their morphological structure evaluated through MEV has shown several differences among the studied biomasses and these characteristics may affect combustion processes.

Different thermal behaviors should be taken into account in the prediction of the hydrodynamic behavior by using different biomass materials as fuels in fluidization processes under high temperature (>500 °C) and atmospheric air condition.

Heat release in function of the different lignocellulosic structures could cause different temperature and gas velocity variations inside the bed, which could affect the fluidization regime in a fluidized bed combustor.

Our results have shown that the predicted values of minimum fluidization velocity ($U_{mf,mix}$) obtained through Eq. (8) have revealed deviations from 1 to 63% related to experimental values. Therefore, such an equation must be cautiously used to predict U_{mf} values for biomass–sand mixtures.

Finally, the physical–chemical properties of the fuel constitute the basis of the choice of a particular technology for the combustion process. Appropriate methods are important for the characterization of these alternative fuels whose features are quite different from those of traditional fuels. Regarding the use of biomass materials, the values widely vary and can result in an extent of concerns including economic, environmental and technical aspects.

Notation

Ar	Archimedes number
$\overline{d}p$	average particle diameter, m
g	gravitational acceleration, m s^{-2}
M	mass, kg
U	superficial velocity, m s^{-1}
x	weight fraction

Greek letters

ε	bulk voidage
μ	gas dynamic viscosity, kg m^{-1} s^{-1}
ρ	gas density, kg m^{-3}
ρ_{bulk}	bulk density of the loosely packed bed, kg m^{-3}
ρ_p	particle density, kg m^{-3}

Subscripts

B	biomass particles
S	sand particles
mf	minimum fluidization
mix	binary mixture

Acknowledgment

The authors are grateful to the National Council for Scientific and Technological Development (CNPq), Coordination for the Improvement of Higher Education Personnel (CAPES) and São Paulo Research Foundation (FAPESP) (Process n. 2012/00639-9) for the financial support provided for this research. The English language review provided by Professor Angela Pregnolato Giampedro is also acknowledged.

References

[1] D.K. Park, S.D. Kim, S.H. Lee, J.G. Lee, Co-pyrolysis characteristics of sawdust and coal blend in TGA and fixed bed reactor, Bioresour. Technol. 101 (2010) 6151–6156.
[2] J.A. Suarez, P.A. Beaton, Physical properties of Cuban coffe husk for use as an energy source, Energy Sources 25 (2003) 953–959.
[3] A. Demirbas, Combustion characteristics of different biomass fuel, Prog. Energy Combust. Sci. 30 (2003) 219–230.
[4] N. Chevanan, A.R. Womac, V.S.P. Bitra, C. Igathinathane, Y.T. Yang, P.L. Miu, S. Sokhansanj, Bulk density and compaction behavior of knife mill chopped switchgrass, wheat straw and corn stover, Bioresour. Technol. 101 (2010) 207–214.
[5] T.R. Rao, J.V.R. Bheemarasetti, Minimum fluidization velocities of mixtures of biomass and sand, Energy 26 (2001) 633–644.
[6] A. Pattiaya, Thermochemical characterization of agricultural wastes from Thai cassava plantations, Energy Sources 33 (2011) 691–701.
[7] W.H. Chen, P.C. Kuo, A study on torrefaction of various biomass materials and its impact on lignocellulosic structure simulated by a thermogravimetry, Energy 35 (2010) 2580–2586.
[8] P. Ghetti, L. Ricca, L. Angelini, Thermal analysis of biomass and corresponding pyrolysis products, Fuel 75 (1996) 565–573.
[9] H. Yang, R. Yan, H. Chen, D.H. Lee, C. Zheng, Characteristics of hemicelluloses, cellulose and lignin pyrolysis, Fuel 86 (2007) 1781–1788.
[10] K. Raveendran, A. Ganesh, K.C. Khilar, Pyrolysis characteristics of biomass and biomass components, Fuel 75 (1996) 987–998.
[11] E. Özgür, S.F. Miller, B.G. Miller, M.V. Kök, Thermal analysis of co-firing of oil shale and biomass fuels, Oil Shale 29 (2012) 190–201.
[12] M.V. Kök, E. Özgür, Thermal analysis and kinetics of biomass samples, Fuel Process. Technol. 106 (2013) 739–743.
[13] F. Fotovat, J. Shabannian, J. Chaouki, J. Bergthorson, Characterization of the fluidization and mixing of binary mixtures containing biomass at low gas velocities, Proceedings of the 13th Int. Conf. on Fluidization — CFB 10, 2011, (Oregon, USA).
[14] M.G. Rasul, V. Rudolph, Fluidized bed combustion of Australian bagasse, Fuel 79 (2000) 123–130.
[15] H. Cui, R. Grace, Fluidization of biomass particles: a review of experimental multiphase flow aspects, Chem. Eng. Sci. 62 (2007) 45–55.
[16] B. Formisani, R. Girimonte, T. Longo, The fluidization process of binary mixtures of solids: development of the approach based on the fluidization velocity interval, Powder Technol. 185 (2008) 97–108.
[17] Y. Zhang, B. Jin, N. Zhong, Experimental investigation on mixing and segregation behavior of biomass particle in fluidized bed, Chem. Eng. Process. Intensification 48 (2009) 745–754.
[18] W. Wendlandt, Thermal Analysis, John Wiley, New York, 1986.
[19] D. Geldart, Types of gas fluidization, Powder Technol. 7 (1973) 285–292.
[20] P.N. Rowe, The effect of pressure on minimum fluidization velocity, Chem. Eng. Sci. 39 (1984) 173–174.
[21] P. Basu, Combustion and Gasification in Fluidized Beds, Taylor and Francis Group, Boca Raton, Florida, 2006. (473 pp.).
[22] G.L. Borman, K.W. Ragland, Combustion Engineering, McGraw-Hill, Boston, 1998, pp. 125–133.
[23] S.N. Oka, Fluidized Bed Combustion, 1st ed., Marcel Dekker Inc., Nova York, 2004, (600 pp.).
[24] F.P. Qian, C.S. Chyang, K.S. Huang, J. Tso, Combustion and NO emission of high nitrogen content biomass in a pilot-scale vortexing fluidized bed combustor, J. Bioresour. Technol. 102 (2011) 1892–1898.
[25] Y. Haseli, J.A. van Oijen, L.P.H. Goey, A detailed one-dimensional model of combustion of a woody biomass particle, Bioresour. Technol. 102 (2011) 9772–9782.
[26] F. Rouquerol, J. Rouquerol, K. Sing, Adsorption by Powders and Porous Solids: Principles, Methodology and Applications, Academic Press, London, 1999.
[27] P.A. Webb, C. Orr, Analytical Methods in Fine Particle Technology, Micromeritics Instrument Corporation, Norcross, 1997.
[28] C. Driemeier, M.M. Oliveira, F.M. Mendes, E.O. Gómez, Characterization of sugarcane bagasse powders, Powder Technol. 214 (2011) 111–116.
[29] Q. Zhang, W. Cai, Enzymatic hydrolysis of alkali-pretreated rice straw by Trichodermareesei ZM4-F3, Biomass Bioenergy 32 (2008) 1130–1135.
[30] I.G. Markovska, L.A. Lyubchev, A study on the thermal destruction of rice husk in air and nitrogen atmosphere, J. Therm. Anal. Calorim. 89 (2007) 809–814.
[31] B.V. Babu, Biomass pyrolysis: a state-of-the-art review, Biofuels Bioprod. Biorefin. 2 (2008) 393–414.
[32] D.K. Shen, S. Gu, B. Jin, M.X. Fang, Thermal degradation mechanisms of wood under inert oxidative environments using DAEM methods, Bioresour. Technol. 102 (2011) (2011) 2047–2052.